Autopilot System for Kiteplane

Makoto Kumon, *Member, IEEE*, Yuya Udo, Hajime Michihira, Masanobu Nagata, Ikuro Mizumoto, *Member, IEEE*, and Zenta Iwai

***Abstract*—This paper proposes an autopilot system for a small and light unmanned air vehicle called Kiteplane. The Kiteplane has a large delta-shaped main wing that is easily disturbed by the wind, which was minimized by utilizing trim flight with drift. The proposed control system for autonomous trajectory following with a wind disturbance included fuzzy logic controllers, a speed controller, a wind disturbance attenuation block, and low-level feedback controllers. The system was implemented onboard the aircraft. Experiments were performed to test the performance of the proposed system and the Kiteplane nearly succeeded in following the desired trajectory, under the wind disturbance. Although the path was not followed perfectly, the airplane was able to traverse the waypoints by utilizing a failsafe waypoint updating rule.**

***Index Terms*—Autopilot, fuzzy control, Kiteplane, unmanned air vehicle (UAV).**

I. Introduction

UNMANNED air vehicles (UAVs) are useful for observing and planning rescue activities in dangerous areas, such as those affected by volcanoes, earthquakes, and fires. From a design perspective, UAVs must have enough payload to carry the necessary equipment, must be able to fly for an extended period of time, and must be small and light enough to be transported easily to the desired launch location. It is especially important for UAVs to be able to fly at low altitudes in order to closely observe the terrain, although they are more likely to crash due to irregular wind or obstacles. Therefore, sophisticated autopilot systems are necessary and UAVs should be designed to crash with minimal damage.

Airplanes boast a long history of automatic control, and many of these control techniques can also be applied to autonomous UAVs. Airplane dynamics are nonlinear, so controllers based on linear theories are not sufficient for trim conditions that have deviated from the nominal trim condition. Several approaches have instituted various robust control methods, such as the H_∞ controller design, gain scheduling techniques, sliding mode control, etc., to overcome this difficulty [2]–[9]. In this paper, a fuzzy control approach is adopted in order to encode skilled operators' suggestions, and methods utilizing fuzzy logic for UAV flight control are proposed. Fernández–Montesinos *et al.* [10] utilized fuzzy logic for guidance and control for an airplane landing under windshear. Vaščák *et al.* [11] adopted a fuzzy logic controller that was originally proposed by Propocyk and Mamdani [12] and Sugeno *et al.* [13] proposed a fuzzy controller for an autonomous helicopter.

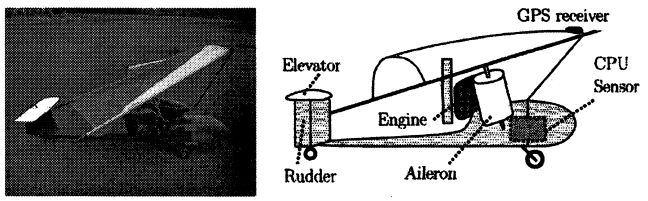

Fig. 1. Kiteplane.

A variety of UAV structures have also been studied. Helicopters have been examined extensively in spite of the complex dynamics required for hovering [13]–[18]. The size and weight of UAVs are also important factors. Grasmeyer and Keennon [19] developed a micro air vehicle (MAV) called Black Widow and Wu *et al.* [20] proposed an MAV whose wingspan was smaller than 4 cm. Deng *et al.* [21] and Schenato *et al.* [22] researched small MAVs that were inspired by insects. Lyshvski [23], [24] studied special control surfaces for MAVs that are essential for small UAVs.

Although many control techniques have been proposed and compact UAVs have been developed, a practical autonomous small and light UAV that can carry a sufficient payload has not yet been widely accepted. This paper develops an autopilot system of a UAV that is small, light, and can also transport a large payload. This UAV is called Kiteplane [25], [26] as its main wing, which is its largest component, is of the shape of a kite-like delta (Fig. 1). The main wing is light and flexible as it is made up of cloth, and thus, it can be large without making the airplane heavy. Although the Kiteplane is light, it is capable of carrying a large payload. The wing's flexibility provides safety and robustness if it crashes into the ground. The center of the mass is located under the main wing and the ailerons are attached at dihedral angles. This configuration results in a stable attitude while the aircraft is in a trim state and provides easily controlled motion. Therefore, the airplane can be controlled by using slow-rate low-cost sensors, such as the global positioning system (GPS), without performing a full attitude measurement. Kumon *et al.* [27] proposed a trajectory-following controller for the Kiteplane based on proportional-integral-derivative (PID) output feedback without using attitude information. Numerical simulations verified that this method is effective when there is no wind disturbance. However, wind disturbance significantly deteriorates the path following performance because of its large

Manuscript received September 28, 2004; revised May 31, 2006. Recommended by Technical Editor J. van Amerongen.

M. Kumon, I. Mizumoto, and Z. Iwai are with the Department of Intelligent Mechanical Systems, Graduate School of Science and Technology, Kumamoto University, Kumamoto 860-8555, Japan (e-mail: kumon@gpo.kumamoto-u.ac.jp; ikuro@gpo.kumamoto-u.ac.jp; iwai@gpo.kumamoto-u.ac.jp).

Y. Udo is with Fuji Xerox Company, Ltd., Mie 519-0393, Japan (e-mail: udo.yuya@fujixerox.co.jp).

H. Michihira is with Nitto Denko Company, Osaka 567-8680, Japan (e-mail: hajime_michihira@gg.nitto.co.jp).

M. Nagata is with the Department of Electronic Control, Kumamoto National College of Technology, Kumamoto 861-1102, Japan (e-mail: nagata@ec.knct.ac.jp).

Digital Object Identifier 10.1109/TMECH.2006.882994

main wing. The dynamics of the Kiteplane are nonlinear and the control inputs are bounded by mechanical limitations. Therefore, simple PID controllers are not sufficient enough under windy situations. Instead, an advanced autopilot system that can attenuate wind disturbances is necessary. Fortunately, some skilled model airplane pilots were able to operate the Kiteplane via radio control, and their instructions on controlling the airplane were available. This *a priori* knowledge is a great help in designing the basic controller structure. The controller according to human operation can be expected to control the airplane as operators do. When the behavior of the controlled system is intuitively predictable by operators, operators are able to find hazardous situations such as system failure easily, and thus can take control of the airplane in such dangerous situations. According to this concept, the human operation was encoded as a control scheme using fuzzy logic [1] and a controller based on this information was designed in this paper, as the fuzzy reasoning is able to model linguistic operators' reasoning quite easily.

A trim flight with drift was considered for attenuating the wind disturbance. To accomplish this goal, the sideslip angle, which is the difference between the direction the airplane is flying and it is heading are controlled to attenuate the wind's effects.

The proposed method was developed and implemented onboard a small all-in-one computer system. Experiments verified the effectiveness of the proposed method, even during wind disturbances.

This paper is organized as follows. In Section II, the Kiteplane and the computer system are introduced. The dynamics of the system are then derived in Section III. The autopilot system is detailed in Section IV and the results of an experiment are presented in Section V. Section VI provides a conclusion.

II. Kiteplane

The Kiteplane's length, wingspan and height are 2280, 2780, and 1130 mm, respectively. It weighs approximately 20 kg and can carry more than a 6-kg payload. The Kiteplane can take off from a runway or a flat field, can fly higher than 3000 m above sea level, and land on the ground. The airplane has five wings: The delta-shaped main wing, two ailerons, an elevator, and a rudder. The main wing is fixed to the body. Servomotors are used as control surface actuators and are attached to the ailerons, the elevator, and the rudder. The engine is mounted in the center of the body and its throttle is also controlled by a servomotor.

The onboard computer system, which will hereafter be referred to as *the CPU*, is a PC/104 IBM-PC compatible embedded PC unit (Advantech, PCM-3370). It is connected to an *A/D unit* (Advantech, PCM-3718 HG), a GPS (Furuno Electric Company, GN-79), and a FPGA system for a servo signal generator/receiver unit. The sensor unit connected to the A/D unit contains three accelerometers (Crossbow, CX02LF3), three gyroscopes (Murata Manufacturing Company, ENV-05F-03), a magnetometer (AP1 System, AM-21 M) for measuring the azimuth angle, and two inclination meters (Midori Precisions, UV-00H) for determining the roll and pitch angles. It is worth noting that only the GPS, the gyroscopes, and the magnetometer are used by the proposed autopilot method. The remaining components are installed for future use. All the servomotors are controlled manually via radio control when the system is in manual mode or automatically by the onboard computer system when the system is in auto mode. A block diagram of the system is shown in Fig. 2.

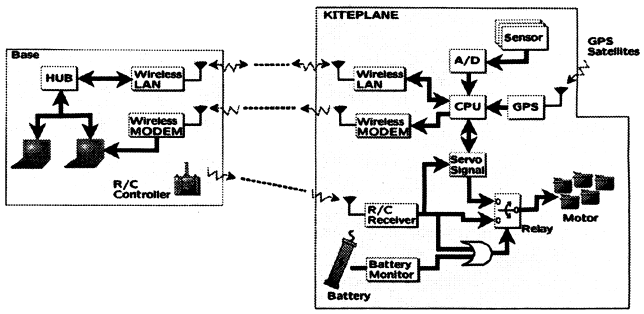

Fig. 2. Overview of the autopilot system.

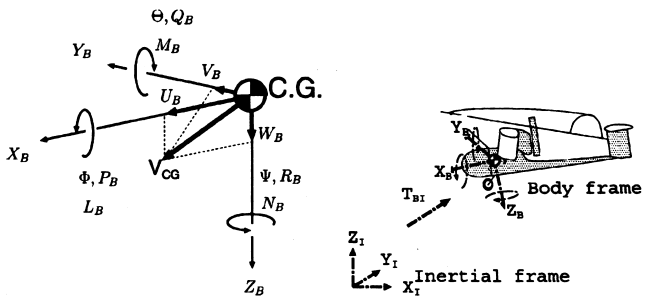

Fig. 3. Body frame and inertial frame.

ART-Linux [28], a real-time operating system based on Linux, was used and the autopilot system was implemented as a real-time task. GPS information was available once per second and other sensory information were sampled every 10 ms.

III. Kiteplane Dynamics

Although the complete dynamics of the Kiteplane are extensively complex, a simple rigid body model can provide useful information. In order to concentrate on the dynamics to be controlled during nominal conditions, Section III considers the case without wind disturbances.

Let the body frame be a Cartesian coordinate system that is attached to the airplane with the origin located at the center of gravity (Fig. 3). The X-axis is aligned with the front of the body and the Z-axis is oriented downward when the airplane is on the ground. The Y-axis is defined using a right-hand coordinate system. Let the inertial frame be a Cartesian coordinate system that is fixed to the ground. The X-axis and the Y-axis of the inertial frame are aligned to the east and the north, respectively. The Z-axis is the perpendicular direction oriented upward. The velocity of the airplane is denoted as V_{CG} and let U_B, V_B, and W_B represent the components of V_{CG} with respect to the body frame.

P_B, Q_B, and R_B represent the angular velocity components with respect to the body frame. $F_{XB}, F_{YB}, F_{ZB}, L_B, M_B$, and N_B represent the aerodynamic forces and moments. The Z–Y–X Euler angle is defined from the inertial frame to the body frame by Φ, Θ, Ψ and the transformation matrix from the inertial frame to the body frame is denoted as $T_{BI}(\Phi, \Theta, \Psi)$, or $\boldsymbol{T}_{BI}$ for short. It is easy to show that there exists an inverse of $\boldsymbol{T}_{BI}$, as long as $\Theta \neq \pm\frac{\pi}{2}$. This inverse will be denoted as $\boldsymbol{T}_{IB}$. m and $\boldsymbol{I}$ are the mass of the airplane and the inertia matrix, respectively. The location of the center of the gravity is represented by X_I, Y_I, Z_I, with respect to the inertial frame.

Let $\boldsymbol{\lambda}_B = [U_B, V_B, W_B]^T$ and $\boldsymbol{\xi}_B = [P_B, Q_B, R_B]^T$. Using the defined notation, the dynamics of the Kiteplane can be written as follows:

$$m\frac{d}{dt}\boldsymbol{\lambda}_B + \boldsymbol{\xi}_B \otimes \boldsymbol{\lambda}_B = \boldsymbol{T}_{BI}\begin{bmatrix}0\\0\\mg\end{bmatrix} + \begin{bmatrix}F_{XB}\\F_{YB}\\F_{ZB}\end{bmatrix} \tag{1}$$

$$I\frac{d}{dt}\boldsymbol{\xi}_B + \boldsymbol{\xi}_B \otimes \boldsymbol{I}\boldsymbol{\xi}_B = \begin{bmatrix}L_B\\M_B\\N_B\end{bmatrix} \tag{2}$$

$$\frac{d}{dt}\begin{bmatrix}X_I\\Y_I\\Z_I\end{bmatrix} = \boldsymbol{T}_{IB}\boldsymbol{\lambda}_B \tag{3}$$

$$\frac{d}{dt}\begin{bmatrix}\Phi\\\Theta\\\Psi\end{bmatrix} = \begin{bmatrix}\frac{C_\Psi}{C_\Theta} & \frac{S_\Psi}{C_\Theta} & 0\\ -S_\Psi & C_\Psi & 0\\ C_\Psi\frac{S_\Theta}{C_\Theta} & S_\Psi\frac{S_\Theta}{C_\Theta} & 1\end{bmatrix}\boldsymbol{T}_{IB}\boldsymbol{\xi}_B \tag{4}$$

where $C_\Psi, S_\Psi, C_\Theta, S_\Theta$, and g represent $\cos\Psi, \sin\Psi, \cos\Theta$, $\sin\Theta$, and the gravitational acceleration. $\otimes$ denotes the outer product. Since the aerodynamic forces and moments are primarily caused by the wings, $F_{XB}, F_{YB}, F_{ZB}, L_B, M_B$, and N_B are not only functions of the airplane's state, but also functions of the control inputs, which are denoted by $\boldsymbol{u}$ [25], [26], [29].

As is typical in airplane dynamics, the linearized system of the dynamics (1)–(4) can be decomposed into two subsystems: A longitudinal system and a lateral system [26]. The inputs for the longitudinal system are the engine's throttle and the elevator, while the inputs for the lateral system are the aileron and the rudder. Therefore, the autopilot system discussed in Section IV is also divided into two parts that correspond with these subsystems. It is worth noting that because $\boldsymbol{u}$ are bounded, the limitation makes it impossible to directly cancel the effect of the disturbances.

IV. Autopilot System

This section first defines the objective of autonomous flight and then proposes the autopilot system to achieve this objective. As wind disturbances can greatly affect the motion of airplanes that have large wings and fly at low Mach numbers, such as the Kiteplane, trim flight with drift is considered to attenuate the effects of the wind disturbance.

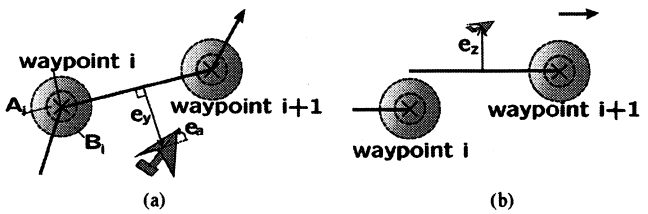

Fig. 4. Reference path. (a) Lateral reference. (b) Longitudinal reference.

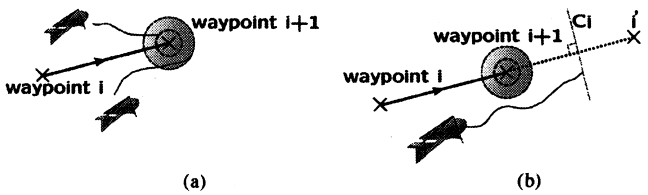

Fig. 5. Target point update. (a) Case I. (b) Case II.

A. Reference Path and Target Updating Rules

For simplicity, the reference path for the airplane is defined as lines connecting specified waypoints. The reference path is graphically depicted in Fig. 4. As the controller is divided into two subsystems, the reference path is divided into a lateral plane containing latitude and longitude [Fig. 4(a)] and a longitudinal plane containing altitude [Fig. 4(b)]. Only one waypoint, called the target point, is considered at a time and the reference path is defined as the line extending from the previous to the current target points. The target point is updated when the airplane *passes* the previous target point, as discussed later.

Let e_y, e_a, and e_z represent the horizontal displacement from the nearest point on the reference path to the horizontal position of the airplane, the difference from the desired direction defined in Section IV-B to the heading of the airplane, and the difference in altitude from the level longitudinal reference path to the altitude of the airplane, respectively.

Each waypoint is surrounded by two concentric regions denoted as A_i and B_i in Fig. 4. The airplane is said to have *passed* the target point when it enters the small region A_i. Under wind disturbance, however, the airplane may not be able to enter region A_i. A weak target updating criterion is introduced for these unexpected situations. In this case, the target should be updated when the airplane leaves region B_i after it has entered B_i. These two cases are summarized in Fig. 5(a).

It is considered a failure if the airplane approaches the target point after flying a distance C_i along the reference path without entering region B_i [Fig. 5(b)]. In this case, the airplane is required to turn back toward the target. To achieve this task, the previous target point is mirrored across a symmetry plane defined at the current target point and a new reference path is defined as the line from the mirrored target point to the current target point.

B. Autopilot System

The structure of the proposed autopilot system is shown in Fig. 6. There are three fuzzy logic controllers (FLCs) incorporated into the system. One controller is employed by the

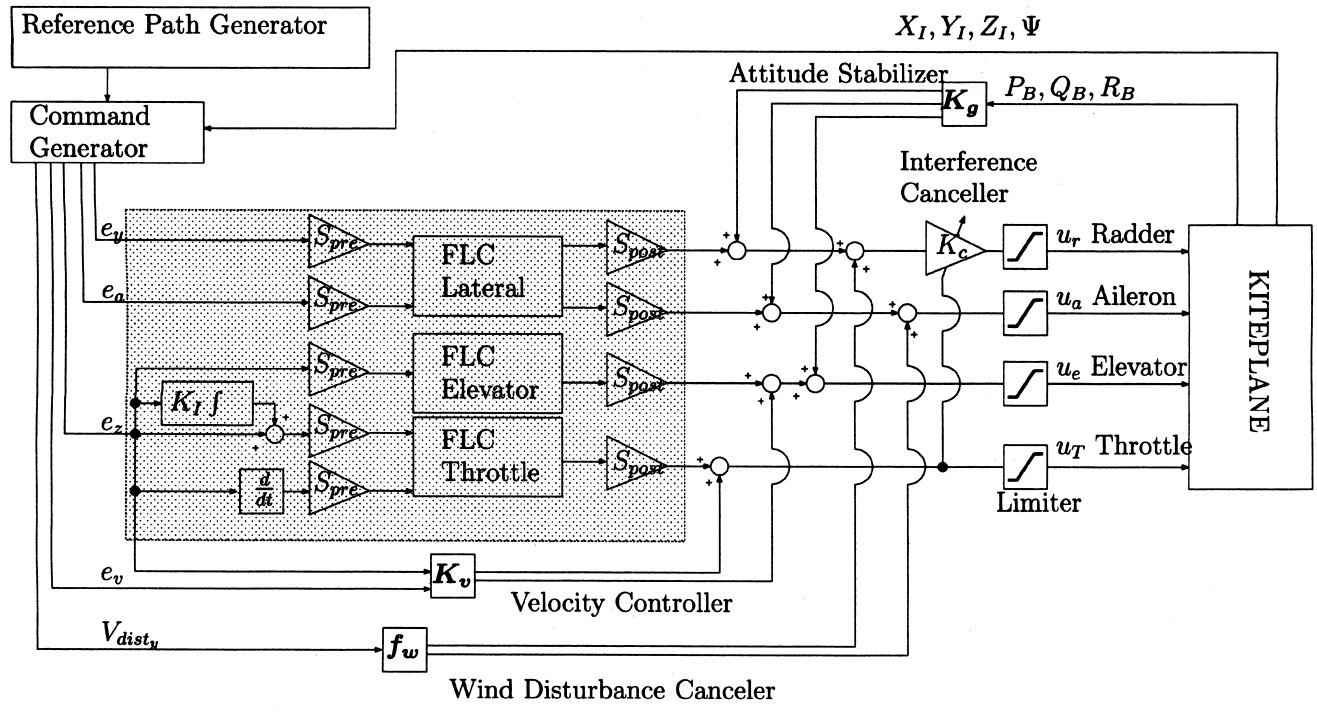

Fig. 6. Block diagram of the autopilot system.

lateral system and two are employed for the longitudinal system. The system also contains a wind disturbance attenuation compensator, a velocity compensator, a variable gain (K_c) to suppress interference between the throttle and the rudder, and the direct feedback of the angular velocities measured by the gyros for attitude stabilization. Servo commands are saturated inside the control system and take the actuator's limitations into account.

1) Lateral System: The lateral controller manages the aileron and rudder based upon e_y and e_a to control yaw and roll angle of the airplane. Initially, e_y and e_a are scaled and mapped into fuzzy values. The fuzzy values are denoted as PH, PB, PM, PS, Z, NS, NM, NB, and NH where P, N, Z, H, B, M, and S represent positive, negative, zero, huge, big, medium, and small, respectively. PH and NH are only used for e_a. Each membership function is defined to have a triangular form. Let the output of the FLC be u^*. Rule k is expressed as

Rule k : if e_y is A_k and e_a is B_k then u^* is C_k

where A_k, B_k, and C_k represent the fuzzy values for rule k. These rules are summarized in Table I. The consequences are aggregated by a min − max operation and u^* is defuzzified by employing the centroid method. The defuzzified output is then scaled to fit within the range of the motor command.

The FLC output for the aileron and rudder are $u^{\mathrm{a}}_{\mathrm{FLC}}$ and $u^{\mathrm{r}}_{\mathrm{FLC}}$, respectively. The computation sequence is as

$$u^{\mathrm{a}}_{\mathrm{FLC}} = S^{\mathrm{a}}_{\mathrm{post}} FLC_{\mathrm{lat}} S^{\mathrm{a}}_{\mathrm{pre}}(e_y, e_a)$$
$$u^{\mathrm{r}}_{\mathrm{FLC}} = S^{\mathrm{r}}_{\mathrm{post}} \mathrm{FLC}_{\mathrm{lat}} S^{\mathrm{r}}_{\mathrm{pre}}(e_y, e_a). \quad (5)$$

Here, $\mathrm{FLC}_{\mathrm{lat}}$, $S^{\mathrm{a}}_{\mathrm{pre}}$, $S^{\mathrm{r}}_{\mathrm{pre}}$, $S^{\mathrm{a}}_{\mathrm{post}}$, and $S^{\mathrm{r}}_{\mathrm{post}}$ represent the fuzzy logic reasoning for the lateral system, including the fuzzifier, the defuzzifier, the aileron prescaler, the rudder prescaler, the aileron postscaler, and the rudder postscaler, respectively.

TABLE I
FUZZY LOGIC CONTROLLER RULE SET FOR THE LATERAL PLANE

		e_y						
		NB	NM	NS	Z	PS	PM	PB
e_a	NH	PB	PB	PB	PB	PM	PM	PS
	NB	PB	PB	PB	PS	PM	PS	Z
	NM	PB	PB	PB	PS	PS	Z	NS
	NS	PB	PM	PM	PS	Z	NS	NM
	Z	PM	PM	PS	Z	NS	NM	NM
	PS	PM	PS	Z	NS	NM	NM	NB
	PM	PS	Z	NS	NS	NB	NB	NB
	PB	Z	NS	NM	NS	NB	NB	NB
	PH	NS	NM	NM	NB	NB	NB	NB

2) Longitudinal System: The longitudinal controller generates the commands for the elevator and the throttle. The augmented altitude error is defined as

$$\tilde{e}_z(t) = e_z(t) + K_I \int_{t-T_I}^{t} e_z(\tau)\, d\tau \quad (6)$$

where K_{I} and T_{I} represent a positive gain and an integrating period, respectively. Let the fuzzy logic block output for the elevator and throttle be u^*_{elev} and u^*_{thro}, respectively. These fuzzy logic blocks utilize the augmented altitude error and an altitude time derivative that is denoted as $\dot{e}_z$. The membership functions are of triangle form, and $\tilde{e}_z$ and $\dot{e}_z$ are scaled by $S^{\mathrm{e}}_{\mathrm{pre}}$ and $S^{\mathrm{T}}_{\mathrm{pre}}$, respectively. Then, these values are fuzzyfied into fuzzy values. Similar to the lateral controller, the fuzzy rules are *stipulated* as

TABLE II
FUZZY LOGIC CONTROLLER RULE SET FOR THE ELEVATOR

$\tilde{e}_z$	NB	NM	NS	Z	PS	PM	PB
u_e	NB	NM	NS	Z	PS	PM	PB

TABLE III
FUZZY LOGIC CONTROLLER RULE SET FOR THE THROTTLE

		$\tilde{e}_z$						
		NB	NM	NS	Z	PS	PM	PB
$\dot{e}_z$	NB	PB	PB	PS	PS	PS	NM	NM
	NM	PB	PB	PS	Z	Z	NM	NB
	NS	PB	PB	PS	Z	Z	NM	NB
	Z	PB	PM	PS	Z	NS	NM	NB
	PS	PB	PM	Z	Z	NS	NB	NB
	PM	PB	PM	Z	Z	NS	NB	NB
	PB	PM	PM	NS	NS	NS	NB	NB

Rule k
Elevator: if $\tilde{e}_z$ is $A_{k,\mathrm{elev}}$ then u^*_{elev} is $C_{k,\mathrm{elev}}$
Throttle: if $\tilde{e}_z$ is $A_{k,\mathrm{thro}}$ and $\dot{e}_z$ is $B_{k,\mathrm{thro}}$
then u^*_{thro} is $C_{k,\mathrm{thro}}$

where $A_{k,\mathrm{elev}}, A_{k,\mathrm{thro}}, B_{k,\mathrm{thro}}, C_{k,\mathrm{elev}}$, and $C_{k,\mathrm{thro}}$ represent the fuzzy values of Rule k. The rule sets for the longitudinal system are displayed in Tables II and III. As a small variation in the elevator position can drastically change the trim condition, the elevator command is limited to a small value. Instead, the throttle is primarily used to control the altitude. NB and PB are set to a nearly idling condition and the full-power state of the engine, respectively. As the engine's thrust depends upon the altitude, air density, temperature, and other factors, the integrated error in (6) is utilized to eliminate the offset.

The FLC output for the elevator and throttle are denoted as $u^{\mathrm{e}}_{\mathrm{FLC}}$ and $u^{\mathrm{T}}_{\mathrm{FLC}}$, respectively. The fuzzy reasoning is computed in the same way as for the lateral system, and this case can be summarized as follows:

$$u^{\mathrm{e}}_{\mathrm{FLC}} = S^{\mathrm{e}}_{\mathrm{post}}\mathrm{FLC}_{\mathrm{elev}}S^{\mathrm{e}}_{\mathrm{pre}}(\tilde{e}_z)$$
$$u^{\mathrm{T}}_{\mathrm{FLC}} = S^{\mathrm{T}}_{\mathrm{post}}\mathrm{FLC}_{\mathrm{thro}}S^{\mathrm{T}}_{\mathrm{pre}}(\tilde{e}_z, \dot{e}_z). \quad (7)$$

Here, $S^{\mathrm{e}}_{\mathrm{pre}}, S^{\mathrm{T}}_{\mathrm{pre}}, S^{\mathrm{e}}_{\mathrm{post}}, S^{\mathrm{T}}_{\mathrm{post}}, \mathrm{FLC}_{\mathrm{elev}}$, and $\mathrm{FLC}_{\mathrm{thro}}$ represent the pre- and postscalers and the fuzzy logic reasoning for the elevator and the throttle, respectively.

3) Wind Disturbance Attenuation: Wind disturbance attenuation is essential for the Kiteplane, although, it is difficult to perfectly counteract the effects of the wind with small control inputs. This paper considers a trim flight with drift.

Assume that constant horizontal wind is blowing. The lateral velocity of the airplane and the velocity caused by the wind disturbance are denoted as $V_{\mathrm{CG_I}}$ and V_{dist}, respectively, as depicted in Fig. 7. Recall that U is the X_{B} component of $V_{\mathrm{CG_I}}$ and let V_{dist_y} be the Y_{B} component of V_{dist}. The rotation caused by the wind disturbance is modeled as the angle α_{dist}, with

$$\alpha_{\mathrm{dist}} = \mathrm{a\,tan\,2}(V_{\mathrm{dist}}, U). \quad (8)$$

α_{dist} includes the direction of wind acting on the airplane, which can be utilized to attenuate the disturbance. The desired heading

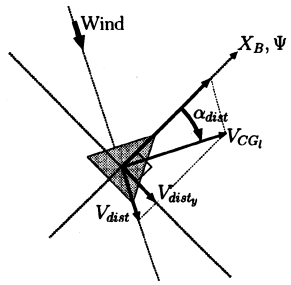

Fig. 7. Wind disturbance.

is defined by adding a counter wind disturbance term to the reference direction

$$\Psi_{\mathrm{d}}(t) = \Psi_{\mathrm{ref}}(i) - \mathrm{sat}(\alpha_{\mathrm{dist}}) \quad (9)$$

where $\Psi_{\mathrm{ref}}(i)$ is the reference path direction to the ith waypoint in the lateral plane and sat is a limiter. From (9), the error e_{a} can be defined as

$$e_{\mathrm{a}}(t) = \Psi(t) - \Psi_{\mathrm{d}}(t). \quad (10)$$

Since the trim condition may also change during a wind disturbance, the following inputs for the rudder and aileron are introduced to maintain the desired heading in spite of the wind:

$$\begin{bmatrix} u^{\mathrm{r}}_{\mathrm{w}} \\ u^{\mathrm{a}}_{\mathrm{w}} \end{bmatrix} = \boldsymbol{f}_w(V_{\mathrm{dist}_y}). \quad (11)$$

In this equation, $\boldsymbol{f}_w$ is a nonlinear vector function that is defined experimentally.

The wind can also disturb the airplane's speed. Therefore, the throttle must be adjusted to maintain the desired flying speed. However, adjusting the throttle also alters the altitude, so the elevator must also be adjusted to simultaneously control the speed and altitude. The speed error e_{v} is defined as follows:

$$e_{\mathrm{v}}(t) = \sqrt{U_{\mathrm{I}}(t)^2 + V_{\mathrm{I}}(t)^2} - V_{\mathrm{d}} \quad (12)$$

where V_{d} represents the desired speed. A linear feedback is adopted for speed control using e_z and e_{v}

$$\begin{bmatrix} u^{\mathrm{e}}_{\mathrm{s}} \\ u^{\mathrm{T}}_{\mathrm{s}} \end{bmatrix} = \boldsymbol{K}_{\mathrm{v}} \begin{bmatrix} e_z \\ e_{\mathrm{v}} \end{bmatrix} \quad (13)$$

where $\boldsymbol{K}_{\mathrm{v}}$ is the feedback gain matrix.

4) Low-level controllers: Apart from the previously mentioned controllers, the autopilot system also contains two low-level controllers.

The angular velocities measured by gyros are fed back to stabilize the rotating motion

$$\begin{bmatrix} u^{\mathrm{a}}_{\mathrm{g}} \\ u^{\mathrm{r}}_{\mathrm{g}} \\ u^{\mathrm{e}}_{\mathrm{g}} \end{bmatrix} = \boldsymbol{K}_{\mathrm{g}}\boldsymbol{\xi}_{\mathrm{B}} \quad (14)$$

where $\boldsymbol{K}_{\mathrm{g}}$ is a negative-definite diagonal matrix.

As the rudder is located behind the propeller, interference occurs between the rudder's and the throttle's control signal.

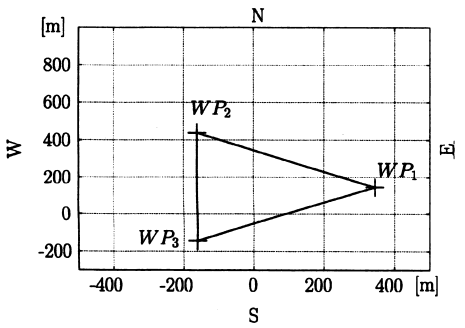

Fig. 8. Lateral reference path.

This may cause the airplane to turn at too steep an angle when the throttle is open. To avoid this, the rudder command is scaled by a variable gain depending upon the throttle command. The gain K_c is defined as

$$K_c = \alpha_C - \beta_C u^e, \tag{15}$$

where u^e represents the throttle command, defined below. α_C and β_C are positive constants.

Summing up, the control commands in (5), (7), and (11)–(15) are restated as follows:

$$\begin{bmatrix} u^a \\ u^r \\ u^e \\ u^T \end{bmatrix} = \text{sat}\left(\begin{bmatrix} u^a_{FLC} + u^a_w + u^a_g \\ K_c(u^r_{FLC} + u^r_w + u^r_g) \\ u^e_{FLC} + u^e_s + u^e_g \\ u^T_{FLC} + u^T_s \end{bmatrix}\right). \tag{16}$$

V. Experimental Results

The proposed autopilot system was implemented in the system described in Section II and experiments were conducted to investigate the performance.

For the experiments, the reference path was defined as a triangle and an overhead view is shown in Fig. 8. In the figure, up points north and the origin represents the initial position of the airplane. WP_1, WP_2, and WP_3 represent the waypoints 1, 2, and 3, respectively. The airplane was directed to pass the waypoints cyclically. The altitude of the runway was 730 m above sea level and the desired altitude for all of the waypoints was 900 m. The desired speed was 6 m/s. The wind was blowing from the southeast at approximately 6–8 m/s during the experiment.

The autopilot system parameters were tuned by both numerical simulations and previous experiments. The parameters are defined as

$$f_w(x) = \text{sat}\left(\begin{bmatrix} -0.3000x^2 + 32.4x + 1.27 \\ -0.0555x^2 + 7.15x + 0.257 \end{bmatrix}\right)$$

$$K_v = -\begin{bmatrix} 5.5 & 0.5 \\ 1.5 & 0.05 \end{bmatrix}$$

$$K_g = -\text{diag}(15, 5, 15)$$

$$\alpha_C = 9.16, \qquad \beta_C = 4.36 \times 10^{-3}.$$

The commands for the servomotors ranged between 1100 and 1900, with 1500 assumed as the neutral position. Unfortunately, there was no clear way to define f_w without a precise dynamical model that would be difficult to identify. Therefore, numerical simulations and experimental data when the operator was ordered to control the airplane under windy conditions were examined and the command signals during the trim flight with drift were extracted. These signals were modeled as second-order polynomials with respect to V_{dist_y} in order to define the actual f_w.

Let the distance from the target i be d_i, calculated as

$$d_i(X, Y, Z) = \sqrt{(X - X_i)^2 + (Y - Y_i)^2 + \frac{1}{4}(Z - Z_i)^2}$$

where X_i, Y_i, and Z_i represent the location of the target i. The installed low-cost GPS module was designed mainly for automobiles and the GPS assumed that the altitude was able to be assumed almost constant in order to enhance horizontal resolution. This assumption works fine for a two-dimensional (2-D) use, but in our experiment, this resulted in the delay of the altitude information. Therefore, the altitude information Z was treated less than other X and Y information as shown in the above criteria d_i. The regions around the target i were defined as

$$A_i : \{(X, Y, Z) \in \boldsymbol{R}^3 | d_i(X, Y, Z) \leq 70\,\text{m}\}$$

$$B_i : \{(X, Y, Z) \in \boldsymbol{R}^3 | d_i(X, Y, Z) \leq 75\,\text{m}\}.$$

Distance C_i was defined to be 100 m for all i.

For the experiments, the airplane was launched in the manual mode and then the autopilot system was turned on. After about a 10-min flight, the autopilot was turned off and the manual mode was used to land the airplane on the runway.

Fig. 9 shows the experimental results of the flight during automode. Fig. 9(a) displays the lateral flight path corresponding to Fig. 8. The figure reveals that the airplane successfully tracked the reference path from waypoint 2 to 3 and from waypoint 3 to 1, but failed from waypoint 1 to 2. Fig. 9(b) shows the airplane's altitude over time. At the beginning of the test, the airplane was at 821.5 m above sea level, which is 78.5 m lower than the reference. However, the airplane reached the reference altitude within 40 s and oscillated around the reference throughout the remainder of the experiment. This behavior was led by the fact that the gain for height control was tuned conservatively since the altitude information by GPS module got delayed, as mentioned earlier. The oscillation was caused at each turn and not by the instability of the system, which was validated by another experiment. Therefore, the result of altitude control was able to be concluded as acceptable. Next, the speed is shown in Fig. 9(c). It was successfully maintained near the reference speed of 6 m/s, except for four peaks that correspond to intervals when the airplane was flying from waypoint 1 to 2.

The airplane's poor performance traveling from waypoint 1 to 2 was caused by the tailwind, which accelerated the airplane up to nearly 20 m/s [Fig. 9(c)]. This speed is more than three times that of the desired speed, so the airplane was required to perform an extremely steep turn to stay on the reference path. However, steep turns are not desirable as they can cause the airplane to fall. The autopilot system was designed to keep the angular velocity small in order to ensure a stable flight. Therefore, it should be

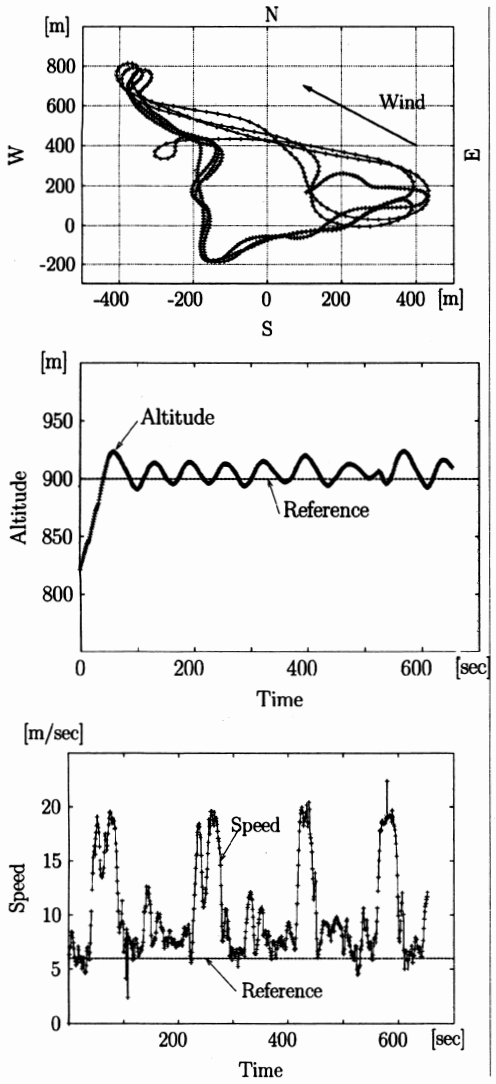

Fig. 9. Flight path and speed.

emphasized that the airplane was able to traverse the waypoints cyclically without losing stability, although it was not able to follow the reference path well due to the tailwind. However, the airplane was able to follow the waypoint updating rule case II. After it initially missed the target, the airplane turned back to pass waypoint 2.

Several features of the experimental results are shown in Fig. 10. Fig. 10(a) displays the distance from the reference path to the position of the airplane. The ▽ signs at the top of the figure represent the moment when the waypoint was updated. The numbers (1–3) represent the waypoint that was targeted. When the target waypoints were updated, the distance changed discontinuously and then converged to zero for target points 1 and 3. When the target point was 2, the distance changed discontinuously as the reference path flipped when the waypoint updating rule case II was activated.

Fig. 10(b-1) and 10(b-2) show the desired airplane's direction and actual information. Zero represents east and the angle

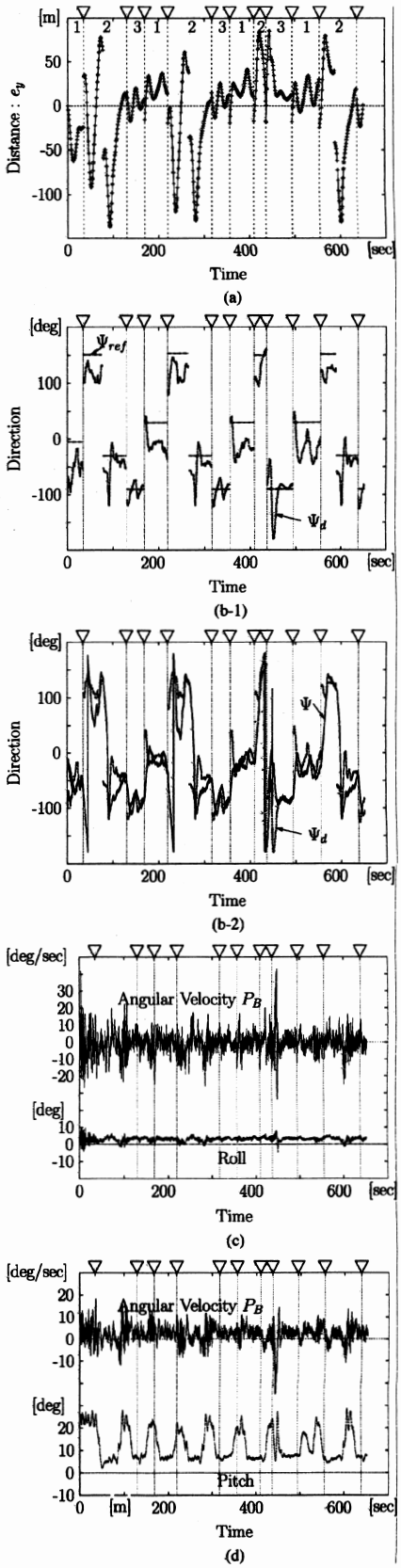

Fig. 10. Error e_y, direction and altitude. (a) Error: e_y. (b-1) Direction: Reference and modified desired direction. (b-2) Modified desired direction and actual direction. (c) Roll. (d) Pitch.

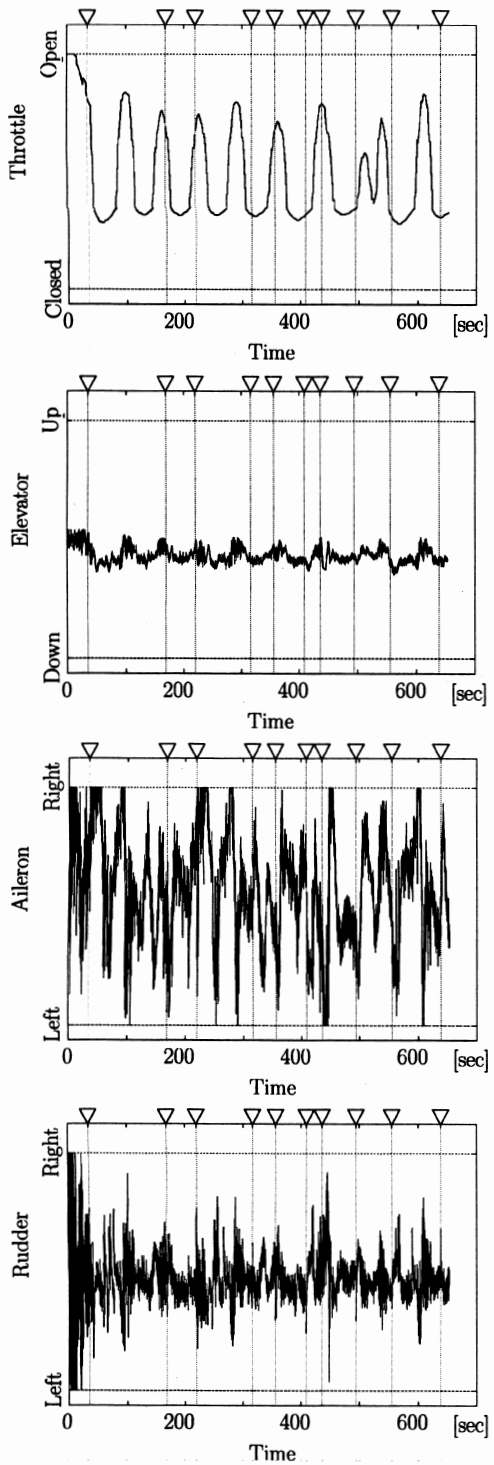

Fig. 11. Control inputs.

increases in the counterclockwise direction. The solid line, the dotted line, and the dashed line represent the heading, the direction of the reference path, and the desired direction computed by the wind attenuation block, respectively. Fig. 10(b-1) shows that the reference path direction and the desired direction were different because of the wind disturbance. Fig. 10(b-2) shows that the heading was controlled well, except for when the airplane experienced the tailwind.

The airplane's roll and pitch are shown in Fig. 10(c) and (d). The angular velocities are shown at the top and the angles are shown at the bottom of the figure. The roll angle was held constant, and the pitch was adjusted up and down depending on the altitude and speed.

Fig. 11 shows the control inputs. As the elevator, rudder, and aileron commands include angular velocity feedback, the high frequency components are shown. Though the aileron input was saturated several times, the saturation did not harm the roll angle performance [Fig. 10(c)].

The controller was tested by other experimental flights with different payloads at different locations and with different desired paths. Although parameters of minor gains were slightly tuned for each test, most of the controller was almost the same, especially fuzzy logic table and wind effect compensator f_w were never modified at all. Throughout those test flights, the system worked fine. This, in turn, concluded the validity of the method.

VI. Conclusion

This paper proposed an autopilot system that used low-cost sensors for a small UAV called the Kiteplane. The Kiteplane has a large main wing and is easily disturbed by the wind, which can be minimized by utilizing trim flight with drift. The proposed control block consists of FLCs, a speed controller, a wind disturbance attenuation block, and low-level feedback controllers. The system was installed onboard the Kiteplane and experiments were conducted to test the performance of the system. The airplane successfully followed the desired path even under wind disturbance.

Due to a tailwind, the path following requirement was not achieved flawlessly, but the airplane was able to traverse the waypoints by utilizing a failsafe waypoint updating rule.

Although the proposed method worked well through various experimental flights, further improvement will make the system more practical. For example, it would be a good challenge to introduce adaptive techniques to tune controller parameters in real time.

Acknowledgment

The authors would like to thank Prof. A. Ohtomo (Kyushu Tokai University, Kumamoto, Japan), K. Okabe, and T. Shigeta (Skyremote Inc., Kumamoto, Japan) for their help in implementing the system and making the test flights.

References

[1] M. Sugeno, *Fuzzy Control* (in Japanese). Tokyo, Japan: Nikkan Kogyo Shinbun, Sep. 1988, pp. 67–136.

[2] M. Lhammash and L. Zou, "Robust aircraft pitch-axis control under weight and center of gravity uncertainty," in *Proc. IEEE Conf. Decision Control*, Dec. 7–10, 1999, vol. 2, pp. 1970–1975.

[3] C. K. Chu, G. R. Yu, and E. A. Jonckheere, "Gain scheduling for fly-by-throttle flight control using neural networks," in *Proc. IEEE Conf. Decision Control*, Dec. 11–13, 1996, vol. 2, pp. 1557–1562.

[4] I. Kaminer, A. M. Pascoal, P. P. Khargonekar, and E. E. Coleman, "A velocity algorithm for the implementation of gain-scheduled controllers," *Automatica*, vol. 31, no. 8, pp. 1185–1191, 1995.
[5] I. Kaminer, A. Pascoal, R. Hallberg, and C. Silvestre, "Trajectory tracking for autonomous vehicles: An integrated approach to guidance and control," *J. Guid. Control Dyn.*, vol. 21, no. 1, pp. 29–38, Jan. 1998.
[6] Y. Shtessel, J. Buffington, and S. Banda, "Multiple time scale flight control using re-configurable sliding modes," in *Proc. IEEE Conf. Decision Control*, Dec. 16–18, 1998, vol. 4, pp. 4196–4201.
[7] R. A. Hess, "Feedback system design for stable plants with input saturation," *J. Guid. Control Dyn.*, vol. 18, no. 5, pp. 1029–1035, 1995.
[8] B. R. Andrievsky and A. L. Fradkov, "UAV guidance system with combined adaptive autopilot," in *Proc. Int. Assoc. Sci. Technol. Dev. Int. Conf. Intell. Syst. Control*, 2003, pp. 91–93.
[9] J. Hauser, S. Sastry, and G. Meyer, "Nonlinear control design for slightly nonminimum phase systems: Application to V/STOL aircraft," *Automatica*, vol. 28, no. 4, pp. 665–679, 1992.
[10] M. A. Fernández-Montesínos, G. Shram, R. Vingerhoeds, H. Vebruggen, and J. A. Mulder, "Windshear recovery using fuzzy logic guidance and control," *J. Guid. Control Dyn.*, vol. 22, no. 1, pp. 178–180, 1999.
[11] K. H. J. Vaščák, P. Kováčik, and P. Sinčák, "Performance-based adaptive fuzzy control of aircrafts," in *Proc. 2001 IEEE Int. Fuzzy Syst. Conf.*, Dec. 2–5, vol. 2, pp. 761–764.
[12] T. J. Propocyk and E. H. Mamdani, "A linguistic self-organizing process controller," *Automatica*, vol. 15, pp. 15–30, 1979.
[13] M. Sugeno, I. Hirano, S. Nakamura, and S. Kotsu, "Development of an intelligent unmanned helicopter," in *Proc. IEEE Int. Fuzzy Syst. Conf.*, Mar. 20–24, 1995, vol. 5, pp. 33–34.
[14] T. J. Koo and S. Sastry, "Output tracking control design of a helicopter model based on approximate linearization," in *Proc. IEEE Conf. Decision Control*, Dec. 16–18, 1998, vol. 4, pp. 3635–3640.
[15] T. J. Koo and S. Sastry, "Differential flatness based full authority helicopter control design," in *Proc. IEEE Conf. Decision Control*, Dec. 7–10, 1999, vol. 2, pp. 1982–1987.
[16] H. Shim, T. Koo, F. Hoffmann, and S. Sastry, "A comprehensive study of control design for an autonomous helicopter," in *Proc. IEEE Conf. Decision Control*, Dec. 16–18, 1998, vol. 4, pp. 3653–3658.
[17] J. Montgomery and G. A. Bekey, "Learning helicopter control through teaching by showing," in *Proc. IEEE Conf. Decision Control*, Dec. 16–18, 1998, vol. 4, pp. 3647–3652.
[18] C. P. Sanders and P. A. Debitetto, "Hierarchical control of small autonomous helicopters," in *Proc. IEEE Conf. Decision Control*, Dec. 16–18, 1998, vol. 4, pp. 3629–3652.
[19] J. Grasmeyer and M. T. Keennon, "Development of the black widow micro air vehicle," in *Proc. IEEE Conf. Decision Control*,, 1998, pp. 3629–3634.
[20] H. Wu, D. Sun, and Z. Zhou, "Micro air vehicle: Configuration, analysis, fabrication, and test," *IEEE/ASME Trans. Mechatronics*, vol. 9, no. 1, pp. 108–117, Mar. 2004.
[21] X. Deng, L. Schenato, and S. Sastry, "Hovering flight control of a micromechanical flying insect," in *Proc. IEEE Conf. Decision Control*, Dec. 4–7, 2001, vol. 1, pp. 235–240.
[22] L. Schenato, D. Campolo, and S. Sastry, "Controllability issues in flapping flight for biomimetic micro aerial vehicles(MAVs)," in *Proc. IEEE Conf. Decision Control*, Dec. 9–12, 2003, vol. 6, pp. 6441–6447.
[23] S. E. Lyshevski, "MEMS smart variable-geometry flexible flight control surfaces: Distributed control and high-fidelity modeling," in *Proc. IEEE Conf. Decision Control*, Dec. 9–12, 2003, vol. 5, pp. 5426–5431.
[24] S. E. Lyshevski, "Distributed control of MEMS-based smart flight surfaces," in *Proc. Amer. Control Conf.*, Jun. 25–27, 2001, vol. 3, pp. 2351–2356.
[25] M. Kumon, K. Eda, M. Nagata, I. Mizumoto, and Z. Iwai, "GPS/IMU attitude estimation of Kiteplane," in *Proc. Int. Symp. Adv. Control Process Syst.*, 2002, pp. 263–268.
[26] M. Nagata, M. Kumon, R. Kohzawa, I. Mizumoto, and Z. Iwai, "Automatic flight path control of small unmanned aircraft with delta-wing," in *Proc. Int. Conf. Control Automat. Syst.*, 2004, pp. 1383–1388.
[27] M. Kumon, M. Nagata, R. Kohzawa, I. Mizumoto, and Z. Iwai, "Flight path control of small unmanned air vehicle," *J. Field Robot.*, vol. 23, no. 3–4, pp. 223–244, 2006.
[28] Y. Ishiwata, T. Matsui, and Y. Kuniyoshi, "Development of Linux with advanced realtime processing feature," in *Proc. 16th Annu. Conf. Robot. Soc. Jpn.*, 1998, pp. 355–356.
[29] R. M. Murray, Z. Li, and S. S. Sastry, *A Mathematical Introduction to Robotic Manipulation*. Boca Raton, FL: CRC Press, 1994.

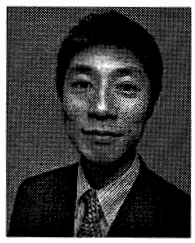

Makoto Kumon (M'00) was born in Yokohama, Japan, in 1972. He received the B.S. degree in applied mathematics and physics, the M.S. degree in applied systems science, and the Ph.D. degree in informatics in 1994, 1996, and 2002, respectively, all from Kyoto University, Kyoto, Japan.

From 2000 to 2005, he was a Research Associate in the Department of Mechanical Engineering and Materials Science, Kumamoto University, Kumamoto, Japan. Currently, he is an Associate Professor in the Department of Intelligent Mechanical Systems at this university. His current research interests include path-following control of robots, auditory robots, and UAV systems.

Dr. Kumon is a member of the Robotic Society of Japan, the Society of Instrument and Control Engineers, the Japan Society of Mechanical Engineers, and the Institute of Systems, Control, and Information Engineers.

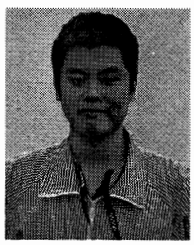

Yuya Udo was born in Kumamoto, Japan, on September 22, 1979. He received the B.S. and M.S. degrees from Kumamoto University, Kumamoto, Japan, in 2002 and 2004, respectively, both in mechanical engineering.

Since 2004, he has been with Fuji Xerox Company, Ltd., Mie, Japan.

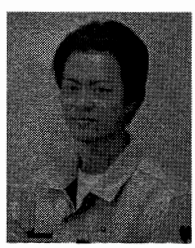

Hajime Michihira was born in Osaka, Japan, on June 17, 1977. He received the B.S. and M.S. degrees from Kumamoto University, Kumamoto, Japan, in 2001 and 2003, respectively, both in mechanical engineering.

Since 2003, he has been with the Nitto Denko Company, Osaka, Japan.

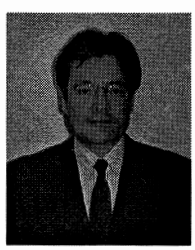

Masanobu Nagata was born in Kumamoto, Japan, on January 1, 1961. He received the B.S. and M.S. degrees in mechanical engineering and the Ph.D. degree in system engineering in 1983, 1985, and 2000, respectively, all from Kumamoto University, Kumamoto, Japan.

From 1985 to 1988, he was with Fuji Electric Corporation, Tokyo, Japan. From 1989 to 2002, he was a Researcher at the Applied Electronic Research Center, Kumamoto Technopolis Foundation (reorganized into Kumamoto Technology and Industry Foundation), Kumamoto. From 2003, he was an Associate Professor. Currently, he is a Professor in the Department of Electric Control, Kumamoto National College of Technology, Kumamoto. Since 1990, he has been engaged in research on automatic control and robotics. His current research interests include automatic flight control systems.

Prof. Nagata is a member of the Japan Society of Mechanical Engineers, the Society of Instrument and Control Engineers, and the Japanese Society for Medical and Biological Engineering.

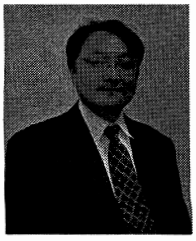

Ikuro Mizumoto (M'02) was born in Yamaguchi, Japan, on November 25, 1966. He received the B.E., M.E., and Dr. Eng. degrees from Kumamoto University, Kumamoto, Japan, in 1989, 1991, and 1996, respectively, all in mechanical engineering.

Since 1991, he has been with the Department of Mechanical Engineering, Kumamoto University, where he is currently an Associate Professor. In 2000, he held a visiting position at the University of Alberta, Edmonton, AB, Canada. His current research interests include adaptive control system design, robust adaptive control, and output feedback-based control for nonlinear systems and their applications.

Prof. Mizumoto is a member of the Japan Society of Mechanical Engineers, the Society of Instrument and Control Engineers, and the Institute of Systems, Control, and Information Engineers.

Zenta Iwai was born in Japan on April 4, 1941. He received the B.E. and M.E. degrees in 1964 and 1996, respectively, both in applied mathematics and physics and the Dr. Eng. degree in control engineering in 1970, all from Kyoto University, Kyoto, Japan.

Since 1970, he has been with Kumamoto University, Kumamoto, Japan. During 2000–2002, he was the Dean of the Faculty of Engineering at this university, where he is currently a Professor in the Department of Mechanical Engineering. He is the author or coauthor of several research papers published in international journals and is the author of several textbooks on control engineering.

Dr. Iwai is a Fellow of the Japan Society of Mechanical Engineers and a Fellow of the Society of Instrument and Control Engineers. He was the recipient of the 2002 Best Educational Publication Award from the Kyushu Association of Engineering Education.